

## Dominant role of grain boundary scattering in the resistivity of nanometric Cu films

Tik Sun,<sup>1</sup> Bo Yao,<sup>1</sup> Andrew P. Warren,<sup>1</sup> Katayun Barmak,<sup>2</sup> Michael F. Toney,<sup>3</sup> Robert E. Peale,<sup>4</sup> and Kevin R. Coffey<sup>1,4</sup>

<sup>1</sup>*Advanced Materials Processing and Analysis Center, University of Central Florida, 4000 Central Florida Boulevard, Orlando, Florida 32816, USA*

<sup>2</sup>*Department of Materials Science and Engineering, Carnegie Mellon University, 5000 Forbes Avenue, Pittsburgh, Pennsylvania 15213, USA*

<sup>3</sup>*Stanford Synchrotron Radiation Laboratory, 2575 Sand Hill Road, Menlo Park, California 94025, USA*

<sup>4</sup>*Department of Physics, University of Central Florida, 4000 Central Florida Boulevard, Orlando, Florida 32816, USA*  
(Received 30 September 2008; revised manuscript received 25 November 2008; published 12 January 2009)

The dominant role of grain boundary scattering in the low-temperature resistivity of both SiO<sub>2</sub> and Ta/SiO<sub>2</sub> encapsulated Cu thin films is demonstrated by the experimental variation and quantification of film thickness, roughness, and grain size. The independent variation in film thickness (28–158 nm) and grain size (35–466 nm) is achieved through subambient temperature film deposition followed by annealing. Experimentally measured film resistivities are compared with both surface scattering and grain boundary scattering models for the classical size effect, showing the dominance of the latter.

DOI: [10.1103/PhysRevB.79.041402](https://doi.org/10.1103/PhysRevB.79.041402)

PACS number(s): 73.63.-b, 73.23.-b, 73.43.Fj, 72.10.Fk

The classical resistivity size effect, wherein conductors with dimensions on the order of the mean-free path of electrons at room temperature (39 nm for Cu) exhibit higher resistivity than bulk conductors, was first noted by Thomson<sup>1</sup> in 1901. The phenomenon was first described by the Fuchs-Sondheimer (FS) (Refs. 2 and 3) theory of surface scattering. The theory, which was derived from the Boltzmann transport equations, attributed resistivity increases in thin films and lines to electron diffuse scattering at the surface with a probability of  $1-p$ , where  $p$  is the specular scattering coefficient. A number of researchers<sup>4,5</sup> took issue with Fuch's assumption of constant specularly for the electron and interface interactions, which ignores electron wavelength, incident angle, and interface roughness. For example, Soffer<sup>6</sup> proposed an alternative surface scattering model based on flux conservation that attributes the resistivity size effect mostly to electrons incident onto rough surfaces at nongrazing angles. In 1970, Mayadas and Shatzkes<sup>7</sup> (MS) proposed an alternative resistivity model, which treats grain boundary scattering as the primary mechanism for the resistivity increase with decreasing conductor thickness. The MS theory, also derived from the Boltzmann transport equations, treats each grain boundary as an internal surface. When an electron collides with a grain boundary, it has a probability of transmission or reflection that is quantified by a reflection coefficient,  $R$  ( $0 < R < 1$ ).

Despite the availability of several models for the resistivity of thin metal conductors, a precise measurement of the relative contribution of surface scattering and grain boundary scattering to the classical size effect is still lacking, and hence there is no consensus on the relative importance of these effects. The measurement difficulty lies in the fact that both surface scattering and grain boundary scattering share a similar geometric dependence, namely, that they are inversely proportional to sample thickness ( $d$ ) and grain size ( $g$ ), respectively, and that the grain size in a series of similarly processed thin-film samples is experimentally observed to scale in proportion to film thickness, i.e., these two parameters are not independent variables in polycrystalline thin films.<sup>7</sup> The presence of roughness at the surface further com-

plicates the matter. While some researchers believe that the resistivity of a rough surface can be larger than a fully diffusive smooth surface described by Fuchs<sup>8</sup> and Sondheimer,<sup>9</sup> others believe that the Fuchs model with  $p=0$  is the upper limit of resistivity resulting from surface and roughness scattering.<sup>6</sup> A significant number of experimental works have attempted to tackle the classical size effect problem, but they all suffer from a lack of quantification and independent variation in the structural characteristics of the films or lines in terms of grain size and thickness.<sup>10–12</sup>

In our previous work,<sup>13</sup> the room-temperature resistivities of SiO<sub>2</sub>/Cu/SiO<sub>2</sub> samples with experimental variation in both sample grain size and film thickness were investigated and the MS model was used to describe the room-temperature resistivities. In this work, we extend our experimental study to low-temperature (4.2 K) resistivities. We also quantify the roughnesses of the upper and lower film surfaces, and we study two types of scattering interfaces, both SiO<sub>2</sub>/Cu/SiO<sub>2</sub> and SiO<sub>2</sub>/Ta/Cu/Ta/SiO<sub>2</sub>. At 4.2 K, the bulk resistivity of Cu is 0.002  $\mu\Omega$  cm (Ref. 14) and the corresponding electron mean-free path is 33  $\mu$ m.<sup>7</sup> To rigorously separate the two effects, we directly measure film thickness, roughness, and grain size and introduce an independent variation in the sample grain size and sample film thickness. This study also includes electron scattering at both a low-resistivity metal or dielectric interface (Cu/SiO<sub>2</sub>) using encapsulated Cu films (SiO<sub>2</sub>/Cu/SiO<sub>2</sub>) and a low-resistivity metal or high-resistivity metal interface (Cu/Ta) using a more complex encapsulation structure (SiO<sub>2</sub>/Ta/Cu/Ta/SiO<sub>2</sub>) to allow comparison of these potentially different surface scattering conditions.

The details of the deposition and annealing of the SiO<sub>2</sub> encapsulated Cu thin-film samples have been previously described<sup>13</sup> and the Ta/SiO<sub>2</sub> encapsulated samples differ only by the addition of a 2 nm Ta layer, dc sputter deposited immediately prior to, and again after, the Cu layer deposition. Table I contains a summary of samples fabricated along with their respective annealing temperature, void area fraction, thickness, root-mean-square roughness of the top ( $r_1$ ) and bottom ( $r_2$ ) Cu/encapsulant interfaces, resistivity, and

TABLE I. Annealing temperature, void area fraction, thickness, root-mean-square roughness (upper,  $r_1$ , and lower,  $r_2$ , of the Cu or encapsulant layer interfaces), resistivity, and grain-size data for (a) SiO<sub>2</sub>-encapsulated Cu thin films and (b) the Ta/SiO<sub>2</sub>-encapsulated Cu thin film. The grain size and void fraction data for samples in (a) are taken from Ref. 13.

(a) (SiO <sub>2</sub> /Cu/SiO <sub>2</sub> )							
Anneal (°C)	Voiding (%)	Thickness (nm)	$r_1$ (nm)	$r_2$ (nm)	$\rho_{at4.2k}$ ( $\mu\Omega$ cm)	Grain diameter (nm)	Grains measured
150	0.1	31.6	1.4	0.8	1.62	40.9 ± 2.4	525
150	0.1	35.3	1.1	1.0	1.30	54.3 ± 2.1	1363
150	1.3	37.1	0.9	0.8	1.14	64.8 ± 2.5	1362
150	0.0	45.1	1.0	0.8	0.90	101.1 ± 4.6	919
150	0.0	71.8	0.6	1.5	0.52	171.8 ± 7.9	872
150	0.2	136.7	N/A	N/A	0.30	344.2 ± 20.2	525
150	0.0	143.9	0.9	1.3	0.25	248.1 ± 17.2	412
400	2.1	41.7	1.0	0.7	0.95	87.7 ± 3.2	1563
400	1.4	83.6	0.6	1.1	0.36	221.5 ± 10.7	785
400	0.0	157.9	N/A	N/A	0.20	419.3 ± 21.8	662
600	2.4	33.6	0.2	0.7	0.92	68.4 ± 4.4	452
600	1.9	36.9	0.5	1.0	0.78	81.4 ± 4.5	576
600	1.5	46.4	0.4	0.9	0.58	112.6 ± 7.7	419
600	0.9	74.5	0.3	1.0	0.34	220.0 ± 9.5	1045
600	0.6	149.7	0.3	1.2	0.16	465.9 ± 17.2	1520
(b) (SiO <sub>2</sub> /Ta/Cu/Ta/SiO <sub>2</sub> )							
Anneal (°C)	Voiding (%)	Thickness (nm)	$R_1$ (nm)	$R_2$ (nm)	$\rho$ at 4.2 k ( $\mu\Omega$ cm)	Grain diameter (nm)	Grains measured
600	0.0	28.3	0.8	1.1	1.82	34.6 ± 1.5	960
600	0.0	34.2	1.1	1.2	1.75	39.4 ± 1.7	1020
600	0.0	38.7	1.3	1.3	1.68	44.3 ± 2.2	743
600	0.0	48.4	1.0	1.0	0.99	69.6 ± 3.4	776
600	0.0	77.9	1.4	1.2	0.68	110.1 ± 4.6	1129
600	0.0	153.1	0.9	1.5	0.32	345.1 ± 15	1033

grain-size data. The sheet resistance of the samples at 4.2 K was measured by dipping a Van der Pauw geometry four-point probe<sup>15</sup> into liquid helium while using a Keithley 2400 source meter and 2182 nanovoltmeter for data collection. Samples for transmission electron microscopy (TEM) were prepared using a back-etching technique and examined by high angle annular dark field (HAADF) imaging in scanning TEM mode at relatively low magnifications to assess the void fraction present in the film. Moreover, the samples were also examined by hollow cone dark field (HCDF) imaging in TEM mode to provide the highest diffraction contrast for grain-size measurements.<sup>13</sup> For the samples reported in Table I, the void fractions are sufficiently small as to have a negligible effect on sample resistivity.<sup>13</sup> Twin boundaries within grains were excluded as this type of grain boundary has been reported to have a minimal contribution to sample resistivity.<sup>16</sup> The reported grain size is the diameter of the equivalent circle with area equal to the average of the grain areas and the errors on the mean are quoted as  $2\sigma$  values at a 95% confidence level for the given grain population.<sup>17</sup> X-ray reflectivity experiments were performed at the Stan-

ford Synchrotron Radiation Laboratory (SSRL). The Cu film thickness and the roughness of the upper and lower Cu/encapsulant layer interfaces were determined by fitting of the reflectivity data to established models.<sup>18,19</sup> Data were collected on thin-film diffraction beam line 2-1. This beam line is equipped with a Huber 2-circle goniometer, a pair of 1 mm slits as the analyzer,<sup>20</sup> and a He filled sample stage used to decrease the air scattering background. X rays of 1.549 Å were monochromated with a double bounce Si(111) crystal. Two types of scans were performed: specular, where  $\omega = 2\theta/2 = \theta$ , and off specular, where  $\omega = 2\theta/2 \pm 0.15^\circ$ . The off-specular scans were used to subtract the contribution of diffusely scattered x rays to the specular reflection resulting in a purely specular reflectivity pattern. Data were collected from  $2\theta = 0.2^\circ - 12^\circ$ , with a step size of  $0.02^\circ$ ,  $0.01^\circ$ , or  $0.005^\circ$  depending on film thickness.

In order to separate the effect of grain boundary scattering from that of surface scattering, the grain size of the Cu samples should ideally be varied fully independent of film thickness, an example of which is shown by the open circles in Fig. 1. Also shown in the figure (filled circles) is the

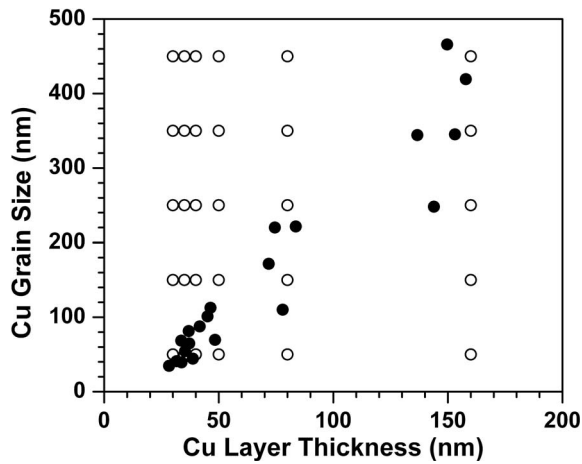


FIG. 1. Plot of grain sizes of Cu thin films as a function of Cu layer thickness. The open circles show an example of an ideal data set without correlation between the two variables and the filled circles are the experimental data from Table I.

measured grain size of the Cu samples (from Table I) as a function of film thickness to illustrate the extent of independent variation that was experimentally feasible in this study. A grain-size variation by a factor of at least 2 is generally available for each sample thickness. With the careful quantification of grain size exercised here, this degree of independent variation is sufficient for the quantification of grain boundary and surface scattering effects.

In Fig. 2(a) the 4.2 K resistivity values (ranging from 0.16 to 1.82  $\mu\Omega$  cm) of the  $\text{SiO}_2/\text{Cu}/\text{SiO}_2$  and  $\text{SiO}_2/\text{Ta}/\text{Cu}/\text{Ta}/\text{SiO}_2$  samples are plotted as a function of thickness. The FS model [Eq. (25) of Ref. 3] shown in the figure fails to describe this variation in resistivity even with the most extreme value for the specularly coefficient ( $p=0$ ), which suggests that surface scattering alone does not explain the resistivity size effect in these Cu thin films. Within the  $\text{SiO}_2/\text{Cu}/\text{SiO}_2$  samples, it can be seen that the sample resistivity decreases with increasing annealing temperature at

similar thicknesses, which agrees with the room-temperature results reported in our previous work.<sup>13</sup> Furthermore, the Cu samples with Ta layers are found to have consistently higher resistivities than those without Ta. As will be shown, the presence of various resistivities at each thickness is a direct consequence of having an extra degree of freedom in grain size (Fig. 1). Figure 2(b) is a plot of the low-temperature resistivity as a function of grain size. It is immediately evident from the figure that the additional variations in resistivity associated with the anneal temperature or the presence of Ta are no longer present, being apparently accounted for by sample grain size, independent of sample thickness. The curve shown in Fig. 2(b) is that of the MS model [Eq. (10) of Ref. 7] with a reflection coefficient of  $R=0.44$  and this provides a much improved fit for sample resistivities. Conclusively, grain size is the dominant resistivity effect.

A variety of more complex models can be used to further explore the roles of surface and grain boundary scatterings in the classical size effect. The sums of the residual squared error for the several models considered in this work are listed in Table II with the optimized fit parameters used. Soffer's model for surface scattering can be used with independent specification of upper and lower interface roughnesses [Eq. (7) of Ref. 21], as is appropriate for this data set, but this is clearly not an improvement over the FS model. Combined models, using Matthiessen's rule, are also considered and included in Table II. The combined FS-MS model allows different specularly coefficients for the Cu/Ta and Cu/ $\text{SiO}_2$  interfaces ( $p_{\text{Ta}}$  and  $p_{\text{SiO}_2}$ , respectively) to be explored but no significant improvement in fit is observed. Among the models listed, the lowest summed residual error is obtained from a combined Soffer-MS model but the extent of improved fit is still not significant over that of the MS model alone. All of the optimized combined models indicate that the average surface scattering contribution for the samples examined is less than 22% of the total resistivity increase. From this we can conclude that the data in Table I provide experimental verification of the MS model, clearly supporting the MS scattering as the dominant effect, and allow, but do not confirm, a weaker surface scattering effect.

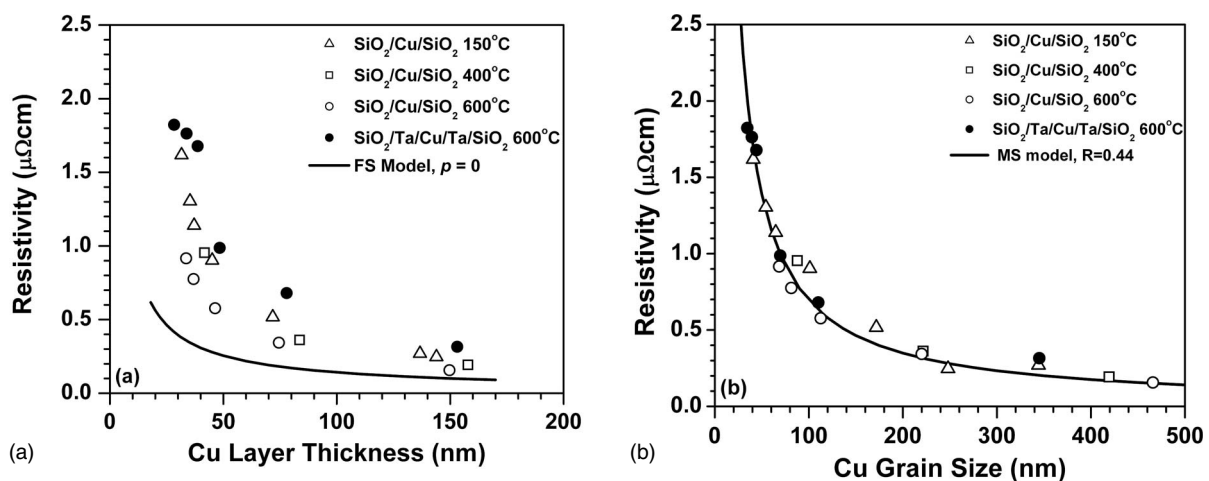


FIG. 2. The resistivity of  $\text{SiO}_2/\text{Cu}/\text{SiO}_2$  and  $\text{SiO}_2/\text{Ta}/\text{Cu}/\text{Ta}/\text{SiO}_2$  thin films (a) as a function of Cu layer thickness and (b) as a function of Cu layer grain size. The data points correspond to the samples listed in Table I. The solid curve corresponds to the FS model in (a) and MS model in (b).

TABLE II. For a series of classical size effect models, the sum of the residual squared error, optimized model parameters, and average relative contributions of surface and grain boundary scatterings to the sample resistivity are given, using the data of Table I. The models examined are the Soffer model (Refs. 6 and 21), the FS model (Refs. 2 and 3), the MS model (Ref. 7), a FS-MS combined model assuming that Cu/Ta and Cu/SiO<sub>2</sub> interfaces scatter similarly, and a FS-MS combined model assuming that Cu/Ta and Cu/SiO<sub>2</sub> interfaces scatter differently.

Model name	Sum square error	Optimized parameters	Surface contribution (%)	Grain boundary contribution (%)
Soffer <sup>a</sup>	17.7	—	100	0
FS	11.4	$p=0$	100	0
MS	0.18	$R=0.44$	0	100
Soffer-MS <sup>a</sup>	0.14	$R=0.42$	11	89
FS-MS	0.16	$R=0.41$ $p=0.44$	17	83
FS-MS (two surfaces)	0.15	$p_{\text{SiO}_2}=0.33$	22	78
		$R=0.40$ $p_{\text{Ta}}=0.21$	18	82

<sup>a</sup>Data set limited to Table I samples with roughness data.

In summary, the contributions of surface scattering and grain boundary scattering and roughness to the resistivity increase observed with reduction in conductor thickness have been carefully studied in polycrystalline Cu thin films through quantitative measurement of the primary experimental variables and the comparison of the data to accepted models for the classical size effect. The samples studied were relatively large grained samples, having an average grain size greater than film thickness. Moreover, we find that grain boundary scattering is the dominant scattering mechanism and that the data presented provide a clear experimental verification of the model of Mayadas and Shatzkes.<sup>7</sup> Additional resistivity effects associated with surface scattering and surface roughness may be present and may have weak contributions to sample resistivity but they cannot be confirmed. Thus, our results show that much of the previous work on the classical resistivity size effect, where data similar to Fig. 1(a) were interpreted as supporting a thickness-based surface

scattering model, may need to be reevaluated. Furthermore, our results suggest that the most effective method of reducing resistivity in thin films for high technology components (e.g., integrated circuits and magnetic recording sensors) is to increase the grain size rather than reduce interface scattering.

We thank S. Roberts and V. Kumar for their assistance with the grain-size data and C. Fredrickson for his assistance with the low-temperature measurements. We gratefully acknowledge the financial support of the Semiconductor Research Corporation, Task No. 1292.008, and our many discussions with colleagues and partial support from the MRSEC program of the NSF under Contract No. DMR-0520425. Portions of this research were carried out at the SSRL, a national user facility operated by Stanford University on behalf of the U.S. Department of Energy, Office of Basic Energy Sciences.

<sup>1</sup>J. J. Thomson, Proc. Cambridge Philos. Soc. **11**, 120 (1901).

<sup>2</sup>K. Fuchs, Proc. Cambridge Philos. Soc. **34**, 100 (1938).

<sup>3</sup>E. H. Sondheimer, Adv. Phys. **1**, 1 (1952).

<sup>4</sup>J. E. Parrott, Proc. Phys. Soc. London **85**, 1143 (1965).

<sup>5</sup>J. M. Ziman, *Electrons and Phonons* (Oxford University Press, London, 1962), pp. 452–460.

<sup>6</sup>S. G. Soffer, J. Appl. Phys. **38**, 1710 (1967).

<sup>7</sup>A. F. Mayadas and M. Shatzkes, Phys. Rev. B **1**, 1382 (1970).

<sup>8</sup>H. Marom and M. Eizenberg, J. Appl. Phys. **99**, 123705 (2006).

<sup>9</sup>S. M. Rossnagel and T. S. Kuan, J. Vac. Sci. Technol. B **22**, 240 (2004).

<sup>10</sup>W. Steinhogel, G. Schindler, G. Steinlesberger, and M. Engelhardt, Phys. Rev. B **66**, 075414 (2002).

<sup>11</sup>H. Marom, J. Mullin, and M. Eizenberg, Phys. Rev. B **74**, 045411 (2006).

<sup>12</sup>W. Wu, S. H. Brongersma, M. Van Hove, and K. Maex, Appl.

Phys. Lett. **84**, 2838 (2004).

<sup>13</sup>T. Sun, B. Yao, A. P. Warren, V. Kumar, S. Roberts, K. Barmak, and K. R. Coffey, J. Vac. Sci. Technol. A **26**, 605 (2008).

<sup>14</sup>D. R. Lide, *CRC Handbook of Chemistry and Physics*, 75th ed. (CRC, Boca Raton, 1994), pp. 12–41.

<sup>15</sup>L. J. Van der Pauw, Philips Res. Rep. **13**, 1 (1958).

<sup>16</sup>L. Lu, Y. Shen, X. Chen, L. Qian, and K. Lu, Science **304**, 422 (2004).

<sup>17</sup>D. T. Carpenter, J. M. Rickman, and K. Barmak, J. Appl. Phys. **84**, 5843 (1998).

<sup>18</sup>M. Wormington, C. Panaccione, K. M. Matney, and D. K. Bowen, Philos. Trans. R. Soc. London, Ser. A **357**, 2827 (1999).

<sup>19</sup>S. K. Sinha, E. B. Sirota, S. Garoff, and H. B. Stanley, Phys. Rev. B **38**, 2297 (1988).

<sup>20</sup><http://www-ssrl.slac.stanford.edu/beamlines/bl2-1/>

<sup>21</sup>J. R. Sambles and K. C. Elsom, J. Phys. D **15**, 1459 (1982).